UCLA
COMPUTATIONAL AND APPLIED MATHEMATICS

A Numerical Investigation of the Interaction Between the Large and Small Scales of the Two-Dimensional Incompressible Navier-Stokes Equations

Gerald L. Browning
William D. Henshaw
Heinz-Otto Kreiss

April 1998

CAM Report 98-23

Department of Mathematics
University of California, Los Angeles
Los Angeles, CA. 90095-1555

A Numerical Investigation of the Interaction between the Large and Small Scales of the Two-Dimensional Incompressible Navier-Stokes Equations

Gerald L. Browning[1]
CIRA, Colorado State University and
NOAA Forecast Systems Laboratory,
Boulder, CO, USA, 80303.

William D. Henshaw[2]
Scientific Computing Group
Los Alamos National Laboratory
Los Alamos, NM, USA, 87545.

Heinz-Otto Kreiss[3]
Department of Mathematics, UCLA
Los Angeles, CA, USA, 90024.

Abstract:
Stability properties of the incompressible Navier-Stokes equations are studied using direct numerical simulations of freely evolving turbulent flow in a two-dimensional periodic box. It is shown that with sufficient resolution an accurate approximation can be computed that converges in the maximum norm. A number of numerical experiments are then performed applying various types of perturbations. From these experiments it is conjectured that the low wave-number modes contained in the initial part of the spectrum (those not yet in the inertial range), are unstable to perturbations but that higher wave-number modes are rather stable. In one case, for example, a large perturbation is added to wave-numbers mid-way through the inertial range. The perturbation is quickly damped and the solution returns close to its unperturbed state. However, since a small amount of energy is transfered to low wave-numbers, the solution eventually begins to deviate from the control run. As further confirmation of the conjecture it is shown that a knowledge of the time history of the low wave-number modes can be used to accurately determine the high wave-number modes for later times. In a computation presented here for Reynolds number 10^5 using 256^2 Fourier modes, the time history of the lowest 8^2 Fourier modes can be used to determine, to a reasonable accuracy, the higher modes. The implication is that if one could accurately measure the time history of the large scale features of a flow then one could possibly compute the small scale features.

[1]Supported by grant N00014-92-J-1089 from the Office of Naval Research.
[2]Supported by grant N00014-95-F-0067 from the Office of Naval Research and by the U.S. Department of Energy through contract W-7405-ENG-36.
[3]Supported by grant N00014-93-1-0551 and N00014-98-1-0125 from the Office of Naval Research.

1 Introduction

Many computations have demonstrated that the incompressible Navier-Stokes equations can be accurately solved using spectral, or higher-order difference methods provided the number of computational modes (number of grid points) is sufficient to resolve the minimum scale of the flow, see for example Browning and Kreiss [4]. The minimum scale is the length scale at which the energy spectrum begins to decay exponentially fast. Therefore, provided the truncation errors are sufficiently small, the numerical solution converges pointwise to a deterministic answer, even for long time-integrations.

Given an accurate solution, the effect of explicitly adding perturbations is studied, in order to try and understand the actual stability properties of the flow. The flow equations are first solved on a two-dimensional periodic box, starting with some smooth initial data for which the Fourier modes have random phases. This flow evolves over time, initially through a complicated state containing many shear layers and then into a state of large vortex structures which persists for long times. This flow behaviour is rather generic as found by many computations [10]. Starting from this *control run*, a number of perturbations are then performed:

- the viscosity coefficient, ν, is changed,
- the viscous operator is altered,
- a high wave-number perturbation is added,
- the time history of the low wave-number modes are specified over time.

The results of these experiments suggest that the very lowest wave-number modes are quite unstable to perturbations but that wave-numbers in the inertial range and higher are surprisingly stable to perturbations. The inertial range represents those intermediate wave-numbers in Fourier space where the energy spectrum, $E(k)$, decays in an algebraic fashion, $E(k) \propto k^{-\beta}$. When perturbations are added to wave-numbers mid-way through the inertial range, for example, the perturbations are quickly damped and the the solution returns close to the unperturbed state. However, since a small amount of energy is slowly transfered to low wave-numbers, the large scale motion eventually deviates from the unperturbed solution.

These results led us to consider the following experiment. Suppose some number of low wave-number modes are fixed to remain equal, at every time step, to their values from the control run and all higher wave-numbers are computed starting from initial values of zero. By fixing the time history of the otherwise unstable low modes, there can be no influence on these low modes from perturbations of the higher modes. It is the found that the high wave-number modes are, to a large degree, regenerated by this process. For example, in a computation reported here of the two dimensional incompressible Navier-Stokes equations, with Reynolds number 10^5 and requiring 256^2 Fourier modes (512^2 grid points) it is found that by specifying the lowest 8^2 modes (8 in each direction), that the the full solution is recovered to a remarkable degree. This process of specifying the low frequencies over time is of course related to the method of data assimilation in meteorology whereby measurements are incorporated into computational simulations, for a description of this approach see, for example, Daley [5].

2 Background: Smallest Scale Estimates

The incompressible Navier-Stokes equations in two or three space dimensions can be written as

$$\mathbf{u}_t + (\mathbf{u}\cdot\nabla)\mathbf{u} + \nabla p = \nu\Delta\mathbf{u} \tag{1}$$

$$\nabla\cdot\mathbf{u} = 0\,. \tag{2}$$

where $\mathbf{u}$ is the velocity, p the incompressible pressure and $\nu > 0$ the kinematic viscosity. Introduce the spatial Fourier coefficients

$$\mathbf{u}(\mathbf{x},t) = \sum_{\mathbf{k}} \hat{\mathbf{u}}(\mathbf{k},t)e^{i\mathbf{k}\cdot\mathbf{x}}\,. \tag{3}$$

and define the (kinetic) energy spectrum $E(k)$ as the amount of energy in modes with $|\mathbf{k}| = k$:

$$\begin{aligned}\text{Kinetic Energy} &= \frac{1}{2}\|\mathbf{u}\|^2 = \frac{1}{2}\sum_{\mathbf{k}}|\hat{\mathbf{u}}(\mathbf{k},t)|^2 \\ &= \sum_k \left\{ \frac{1}{2} \sum_{k-\frac{1}{2}\le|\mathbf{k}|\le k+\frac{1}{2}} |\hat{\mathbf{u}}(\mathbf{k},t)|^2 \right\} \\ &= \sum_k E(k)\ .\end{aligned}$$

Here $\|\cdot\|$ denotes the L_2 norm. There is much evidence to suggest that the energy spectrum $E(k)$ has a power law behaviour over some range of wave numbers, called the inertial range. On a logarithmic plot this inertial range appears as a straight line. Eventually this straight line curves downward when the Fourier coefficients begin to decay exponentially fast. Thus one might expect the following form for the energy spectrum

$$E(k) \propto k^{-\beta} e^{-2\lambda_{\min} k}\|\mathbf{u}(t)\|^2\ . \tag{4}$$

The parameter $\lambda_{\min}$ is called the minimum scale of the flow since $E(k)$ becomes exponentially small for k much larger than $\lambda_{\min}$. The minimum scale is a bound on the size of the smallest eddy or the width of the sharpest shear layer. In [6][7] it was shown that the minimum scale is bounded by the square root of ν divided by the square root of the maximum of the velocity gradients:

$$\begin{aligned}\lambda_{\min} &\ge \sqrt{\frac{\nu}{|D\mathbf{u}|_\infty}}\ , \\ |D\mathbf{u}|_\infty &= \sup_{\mathbf{x}} \sup_{0\le\tau\le t} |\nabla\mathbf{u}(\mathbf{x},\tau)|.\end{aligned}$$

For technical reasons the precise formula for the minimum scale is slightly more complicated than the expression given above. In deriving the bound for $\lambda_{\min}$ in all generality, there are a number of constants that must be estimated at each step in the proof. In principle there could be some large constants involved. For practical purposes, however, the minimum scale is determined by the first few steps in the proof and for these steps the constants are all near 1. Computations confirm that the expression for $\lambda_{\min}$ given above is actually quite accurate in determining how many computational modes are required as shown in section (5).

These results are also true locally in the sense that the minimum scale of the flow over a small region in space and time is determined by the maximum value of $|\nabla\mathbf{u}(\mathbf{x},t)|$ in a slightly larger region [8]. This means that these estimates can be used to locally determine the appropriate mesh spacing for adaptive mesh refinement or they can be used to locally define an "artificial viscosity" to ensure that a numerical solution remains well behaved.

In two dimensional flow the vorticity satisfies a maximum principle, the maximum (minimum) point wise value of the vorticity never increases (decreases). In this case $|D\mathbf{u}|_\infty$ is essentially bounded by it's initial value [6] and then $\lambda_{\min} \propto \sqrt{\nu}$. Thus if the value of ν is decreased by a factor of 4 then the number of computation modes should be increased by a factor of 2 in each space dimension.

In two space dimensions, theories of Batchelor and Kraichnan [1][11] suggest that the decay rate of the spectrum through the inertial range is given by $\beta = 3$ while Saffman predicts $\beta = 4$, [14]. In three dimensions arguments due to Kolmogoroff [13] predict $\beta = -5/3$. For further discussions on the relationships between the smallest scale and the power law behaviour of the spectrum see [6][7].

Our numerical experiments show that the form of $E(k)$ is very stable. From general initial conditions the solution very quickly evolves to a state where the energy spectrum has the form given by equation (4). Furthermore, computations presented here show that the spectrum quickly recovers its form after perturbations are added. The question remains, however, whether the solution itself is stable to perturbations. This question is partially answered by the results of this paper.

3 Numerical Method

The numerical method discretizes the two-dimensional incompressible Navier-Stokes equations written in the vorticity stream-function formulation:

$$\begin{aligned}\xi_t + (u\xi)_x + (v\xi)_y &= \nu\Delta\xi + f \\ \Delta\psi = -\xi, \qquad (u,v) &= (\psi_y, -\psi_x).\end{aligned}$$

The computational domain is taken to be a 2π periodic square. The solution is represented as a truncated Fourier series with w denoting the discrete approximation to the vorticity ξ and $\hat{w}$ denoting the discrete Fourier transform of w:

$$w(x,y,t) = \sum_{k_1=-\frac{1}{2}N+1}^{\frac{1}{2}N-1} \sum_{k_2=-\frac{1}{2}N+1}^{\frac{1}{2}N-1} \hat{w}(k_1,k_2,t) e^{i(k_1 x + k_2 y)}.$$

Similarly the Fourier transform of the stream-function ψ and f are denoted by $\hat{\psi}$ and $\hat{f}$ respectively. The equation for the Fourier coefficient $\hat{w}(k_1,k_2,t)$ is

$$\begin{aligned} \hat{w}_t + ik_1(\widehat{uw}) + ik_2(\widehat{vw}) &= -\nu(k_1^2+k_2^2)\hat{w} + \hat{f} \\ (k_1^2+k_2^2)\hat{\psi} &= \hat{w}. \end{aligned} \tag{5}$$

The convolutions $\widehat{uw}$ and $\widehat{vw}$ (i.e. the Fourier transforms of the products uw and vw) are computed from $\hat{u}$, $\hat{v}$ and $\hat{w}$ by transforming to real space, forming the products and then transforming back to Fourier space, (pseudo-spectral method). The equations (5) are integrated in time using a fourth-order Adams-Bashforth multistep scheme. A Runge-Kutta scheme is used to restart the integration after the time step is changed. For details the reader is referred to [6].

4 Unperturbed control run

Let $w_c(x,y,t)$ denote the vorticity for a *control run* that will be used to compare to various perturbation computations. The initial conditions for the control run are chosen to have random phase and an energy spectrum of

$$E_c(k) = C_c\ k\ e^{-(k/k_a)^2}$$

where $k_a = 3.5$ and the constant C_c is chosen so that the vorticity has a maximum of 1,

$$|w_c(\cdot,\cdot,0)|_\infty = 1.$$

The maximum value of the velocity in this run was about 0.2. Figure (1) shows contours of the vorticity for $\nu = 10^{-5}$; dashed lines representing negative values. From an initially smooth state the solution develops narrow shear layers and small vortices. Eventually the vorticity reorganizes itself into larger coherent structures. Figure (2) displays the vorticity spectrum on a log-log scale and the evolution of some L_2 norms over time. The vorticity spectrum $w(k,t)$ is defined as the average value of $|\hat{w}(\mathbf{k},t)|$ for $|\mathbf{k}| \approx k$,

$$w(k,t) = \frac{\sum_{k-\frac{1}{2}\le|\mathbf{k}|\le k+\frac{1}{2}} |\hat{w}(\mathbf{k},t)|}{\sum_{k-\frac{1}{2}\le|\mathbf{k}|\le k+\frac{1}{2}} 1} \tag{6}$$

The norms plotted are the total kinetic energy, $\mathrm{A} = \frac{1}{2}\|u^2+v^2\|$, the L_2-norm of the vorticity, $\mathrm{B} = \|w\|$, and the rate of dissipation of vorticity

$$\mathrm{C} = \nu^{1/2} J_1 \equiv \nu^{1/2} \left(\|w_x\|^2 + \|w_y\|^2\right)^{1/2}.$$

For plotting purposes the norms are all scaled to have a maximum value of 1. The scale factors are indicated in the figure.

5 Resolved versus under-resolved computations

This section shows how the solution behaves when computed with different resolutions. It will also been demonstrated that the number of grid points (in each space dimension) required to compute an accurate answer is given approximately by the inverse of the minimum scale,

$$N(\nu, |D\mathbf{u}|_\infty) = \frac{1}{\lambda_{\min}} = \left[\frac{|D\mathbf{u}|_\infty}{\nu}\right]^{1/2} \tag{7}$$

The solution is computed for $\nu = 2 \times 10^{-5}$ with $N = 128, 256, 512$. In these computations the maximum norm of the velocity gradients is $|Du|_\infty \approx .9$ From the expression (7) one would estimate that the number of grid points required is

$$N \approx \left[\frac{.9}{2 \times 10^{-5}}\right]^{1/2} \approx 212.$$

The solutions for these runs and the energy spectra are shown in figure (3). It can be seen that with sufficient resolution the solutions converge to a well determined answer. The solutions for $N = 256$ and $N = 512$ are very similar. Note that the position of the contour lines is a very sensitive measure. When the computation is under-resolved the highest wave-number modes become large, instead of decaying to zero. The $N = 256$ run is reasonably accurate even though the spectrum does not decay as much as in the $N = 512$ run. The smallest scale estimate of $N = 212$ provides a good guess of the number of grid points required.

6 Perturbation: Changing the viscosity coefficient ν

The solutions shown in figure (4) illustrate how the solution changes when the viscosity is changed. Starting from the same initial conditions as for the control run, the equations are integrated using $\nu = 10^{-4}$, $\nu = 10^{-5}$ and $\nu = 5 \times 10^{-6}$. Contours of the vorticity are compared at times $t = 100$ and $t = 200$. The figures show that the solutions are quite similar at time 100 although the shear layers are much sharper as the viscosity is decreased. By time 200 there are significant differences between the solutions.

7 Perturbation: Super-viscosity, changing the form of the viscous operator

Super-viscosity, also called hyper-viscosity, consists of changing the dissipation operator from the standard Laplacian,

$$w_t + uw_x + vw_y = \nu \Delta w \tag{8}$$

to a higher order operator such as the Laplacian squared,

$$w_t + uw_x + vw_y = -\nu_4 \Delta^2 w. \tag{9}$$

For a given grid resolution it is possible to solve with a super-viscosity ν_4 which is much smaller than the regular viscosity ν, typically one can take $\nu_4 = \nu^2$. In this way it is possible to solve the equations with dramatically smaller dissipation. Of course one is no-longer solving the Navier-Stokes equations and it is of some interest to know how solutions to (8) compare to solutions to (9). There have been many simulations performed using super-viscosity, see, for example, [2][10].

The initial conditions for the super-viscosity runs are the same as the control run. Figure (5) compares the super-viscosity run to the unperturbed run for a super-viscosity of $\nu_4 = 10^{-9}$. Figure (6) shows the energy spectrum for this run. As can be seen from the figures the solutions are qualitatively similar but quantitatively quite different. Further comparisons can be found in [4],[9].

8 Perturbation: Switched viscosity, changing from regular to super viscosity

There are many possible ways to implement super-viscosity. In this section an attempt is made to design a dissipation that will reproduce the results of standard viscosity but use fewer grid points. One of properties of the Navier-Stokes equations suggested by the results of this paper is that perturbations which affect wave numbers greater than the minimum scale do not have any great effect on the solution. Although the minimum scale is only defined up to a constant, in practice the rule seems to be that perturbations can be added to that portion of the spectrum which is beginning to enter the region of exponential decay (where the spectrum on a log-log plot changes from flat through the inertial range to curving downward).

A dissipation is designed that switches from the Laplacian for low wave numbers to the Laplacian squared for higher wave numbers. In Fourier space this dissipation is defined as

$$\text{dissipation} = \begin{cases} k^2 & \text{for } k^2 < k_0^2 \\ k^4 - k_0^4 + k_0^2 & \text{for } k^2 > k_0^2 \end{cases}$$

Figures (7)-(10) show results of applying the switched viscosity to the control run for $\nu = 10^{-5}$ and $k_0 = 64$ or $k_0 = 128$. When the switch occurs at $k_0 = 64$ there are large changes in the solution. Switching at $k_0 = 128$ has a smaller effect.

9 Perturbation: adding noise to high wave-number modes

In the section (5) it was shown that the solutions to the incompressible Navier-Stokes equations can be accurately computed with enough resolution. This means that small round-off and truncation errors do not have a large effect on the final answer. One may wonder to what degree are the solutions stable to perturbations. In this section some perturbations are made to the high wave-number modes and the change in the solution is measured. It will be seen that these perturbations are quickly damped and the solution returns to be close to its unperturbed value. However, since a small amount of energy is transfered to low wave numbers the perturbed solution eventually begins to deviate significantly from the unperturbed solution for longer times.

Let $w_p(x, y; k_0)$ denote the perturbation to the vorticity that will depend on one free parameter k_0. The perturbation was chosen to have random phase with energy spectrum

$$E_p(k) = C_p e^{-(k-k_0)^2}$$

with the constant C_p chosen so the perturbation $w_p(x, y, k_0)$ has a maximum norm of one,

$$|w_p(\cdot, \cdot; k_0)|_\infty = 1 \ .$$

The perturbation is added to the solution at either at time $t_0 = 0$ or at $t_0 = 50$. The perturbation is centred at mode $k_0 = 64$ or at mode $k_0 = 128$

$$\begin{aligned} w_1(t_0) &= w_c(t_0) + w_p(x, y; k_0 = 32) \\ w_2(t_0) &= w_c(t_0) + w_p(x, y; k_0 = 64) \end{aligned}$$

Figures (16), (18) and (20) compare the unperturbed run to the perturbed run in physical space. Figures (17), (19) and (21) show the spectrum and norms of the evolution of the perturbation over time. This is the difference between the perturbed and the unperturbed solution.

10 Do low modes determine the high modes

The results from the previous section on high wave-number perturbations indicate that there is a small amount of energy that transfers from high wave-numbers to low wave-numbers. This transfer of energy eventually causes the perturbed solution to deviate from the unperturbed solution. It is natural now to ask what will happen if some small number of low wave-number modes are specified in time to be identical with the control run.

The time history of the lowest M^2 wave-numbers from the control run is saved starting from time $t = 50$. The problem is then solved with the lowest M wave-numbers in each space dimension fixed to the values from the control run while the other wave numbers are obtained by solving the Navier-Stokes equations with initial values zero:

$$\begin{aligned} \hat{w}(\mathbf{k}, t) \equiv \hat{w}_c(\mathbf{k}, t) \qquad & |\mathbf{k}| \le M, t \ge 0 \\ \hat{w}(\mathbf{k}, 0) = 0 \qquad & |\mathbf{k}| > M, t = 0 \\ \hat{w}_t + ik_1(\widehat{uw}) + ik_2(\widehat{vw}) = -\nu(k_1^2 + k_2^2)\hat{w} \qquad & |\mathbf{k}| > M, t > 0 \end{aligned}$$

In practice this scheme is implemented by first advancing all modes one time step using the standard program. The values of $\hat{w}$ for the lowest wave-numbers are then over-written using the results saved from the unperturbed run.

Figures (11),(12) show the results from specifying the lowest 8^2 modes (8 modes in each direction) over time. Note how the magnitude of the vorticity and the fine scale structure is recovered to a significant degree. Figures (13),(14) show the results from specifying the lowest 4^2 modes over time. In this case the solution does not agree as well with the control run as in the previous case.

For comparison the results shown in figure (15) indicate the solution that is obtained when the initial conditions are chosen equal to the lowest 4^2 modes from the control run at $t = 50$. The solution is computed in the normal way, with all modes computed by the pseudo-spectral method.

11 Shallow water equations

The shallow water equations with a beta-plane approximation to the coriolis force can be written in the form

$$u_t + uu_x + vu_y + \frac{1}{R_0}(p_x - v) = \nu\Delta u$$
$$v_t + uv_x + vv_y + \frac{1}{R_0}(p_y + u) = \nu\Delta v$$
$$p_t + up_x + vp_y + (P_0 + p)(u_x + v_y) = 0$$

where the Rosby number is $R_0 = \frac{1}{10}$ and the mean pressure is $P_0 = 1$.

Solutions to the shallow water equations can contain fast moving sound waves. The sound waves satisfy a basically linear wave equation and, if present, remain essentially independent from the slower motions [12]. In these computations the sound waves are not of interest so the bounded derivative principle is used to choose initial data to suppress them [3]. Indeed, the stability of the sound waves will follow linear theory to a good approximation.

The initial conditions for the stream function in Fourier space is taken to have amplitude

$$|\hat{\psi}(\mathbf{k}, 0)| = \frac{1}{K[1 + (\frac{k}{k_0})^4]}, \qquad k_0 = 6.$$

with random phase. The constant K is chosen so that the maximum value of the vorticity is one. The initial pressure field is computed from the balance equation

$$\Delta p = R_0 \left[u_x^2 + 2u_y v_x + v_y^2\right] + u_y - v_x$$

This initialization will reduce the amplitude of the sound waves. The shallow water equations are solved numerically with the pseudo-spectral method in space. The time differencing uses leap-frog with the diffusion terms lagged in time for stability. For further details see [4].

The equations are solved with $\nu = 10^{-4}$ and 64^2 Fourier modes (128^2 grid points). Figure (22) shows the results from comparing the unperturbed control run with the run where the the lowest 8 modes are specified over time. It can be seen that the shallow water equations exhibit a similar behaviour to the incompressible equations.

12 Conclusions

Computations presented in this paper demonstrate some surprising stability properties of the two dimensional incompressible Navier-Stokes equations and the shallow water equations. The solutions are quite stable to perturbations at wave-numbers within the inertial range. However, it appears the very lowest modes are quite unstable to perturbations. If some relatively few number of low wave-number modes are fixed over time then much of the high wave-number information can be recovered by solving for all wave-numbers other than the known low modes. It is of some interest as to whether the results observed here will be similar in the three dimensional case. Initial three dimensional computations by Dr. Jacob Yström indicate that this seems to be true. These three-dimensional results will be reported in a future paper.

References

[1] G.K. Batchelor, *Computation of the Energy Spectrum in Homogeneous Two-Dimensional Turbulence,* Phys. Fluid. Suppl. **II** (1969), pp. 233-239.

[2] R. Benzi, G. Paladini, S. Patarnello, P. Santangelo, A. Vulpiani, *Intermittency and Coherent Structures in Two-Dimensional Turbulence,* J. Phys. A: Math. Gen. **19** (1986), pp. 3771-3784.

[3] G. Browning and A. Kasahara and H.-O. Kreiss, *Initialization of the Primitive Equations by the Bounded Derivative Method,* Journal of Atmospheric Sciences, **7**, 37, 1424–1436, 1980.

[4] G.L. Browning and H.-O. Kreiss, *Comparison of Numerical Methods for the Calculation of Two-Dimensional Turbulence,* Mathematics of Computation, **52**, 369–388, 1989.

[5] R. Daley, *Atmospheric Data Analysis,* Cambridge University Press, 1991.

[6] W.D. Henshaw, H.O. Kreiss and L.G. Reyna, *On the smallest scale for the incompressible Navier-Stokes equations*, Theoretical and Computational Fluid Dynamics, **1**, 1–32, 1989.

[7] W.D. Henshaw and H.-O. Kreiss and L.G. Reyna, *Smallest scale estimates for the incompressible Navier-Stokes equations*, Arch. Rational Mech. Anal., **112**, pp. 21–44, 1990.

[8] W.D. Henshaw and H.-O. Kreiss and L.G. Reyna, *Estimates of the Local Minimum Scale for the Incompressible Navier-Stokes Equations*, Numerical Functional Analysis and Optimization, **16(3&4)**, 315–344, 1995.

[9] W.D. Henshaw and H.-O. Kreiss, *A Numerical Study of the Propagation of Perturbations in the Solutions of the 2D Incompressible Navier-Stokes Equations*, Third International Conference on Hyperbolic Problems, B. Engquist and B. Gustafsson, editors, Chartwell-Bratt, 54–61, 1991.

[10] J.R. Herring, J.C. McWilliams, *Comparison of Direct Simulation of Two Dimensional Turbulence with Two-Point Closure: the Effects of Intermittency*, J. Fluid Mech.,**153** (1985), pp. 229-242.

[11] R. Kraichnan, *Inertial Ranges in Two Dimensional Turbulence*, Phys. Fluids, **10** 1967), pp. 1417-1423.

[12] H.-O. Kreiss and J. Lorenz and M.J. Naughton, *Convergence of the Solutions of the Compressible to the Solutions of the Incompressible Navier-Stokes Equations*, Advances in Applied Mathematics, **12**, 187–214, 1991.

[13] A.N. Kolmogoroff, C.R.Acad.Sci. U.S.S.R. **30** (1941), pp. 301.

[14] P.G. Saffman, *On the Spectrum and Decay of Random Two Dimensional Vorticity Distributions at Large Reynolds Numbers*, Studies Appl. Math., **50** (1971), pp. 377-383.

List of Figures

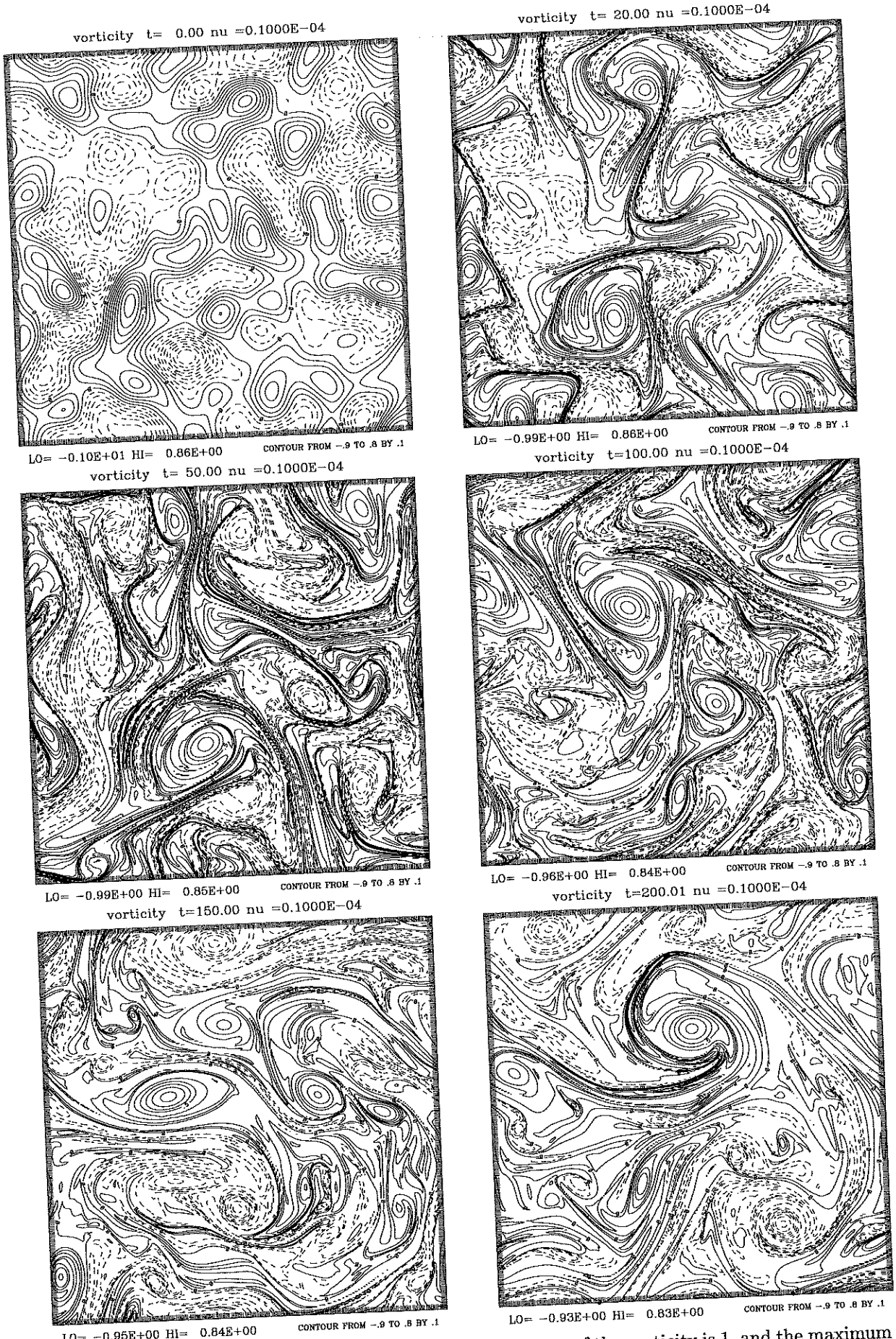

Figure 1: Unperturbed base run, w_b, $\nu = 10^{-5}$. The maximium of the vorticity is 1. and the maximum of the velocity is about .2.

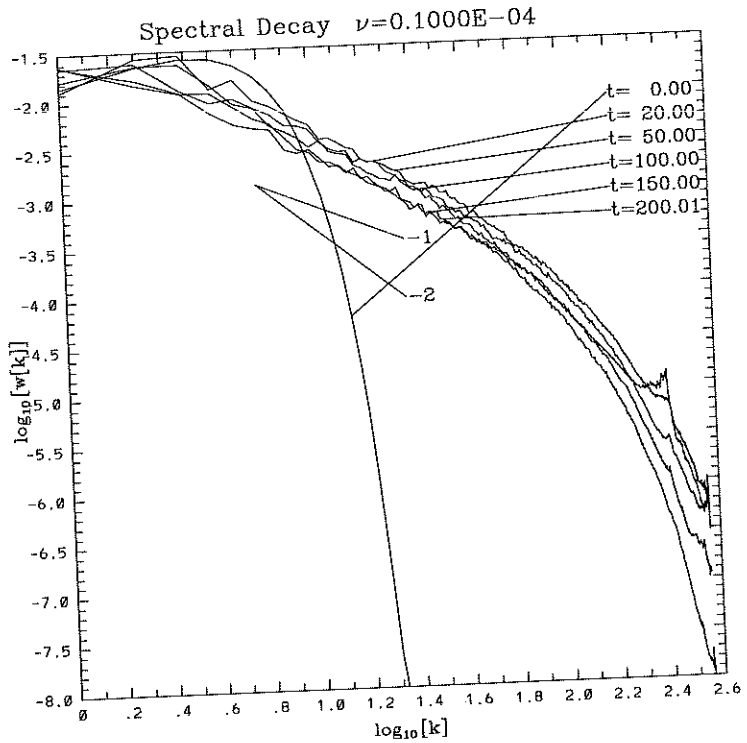

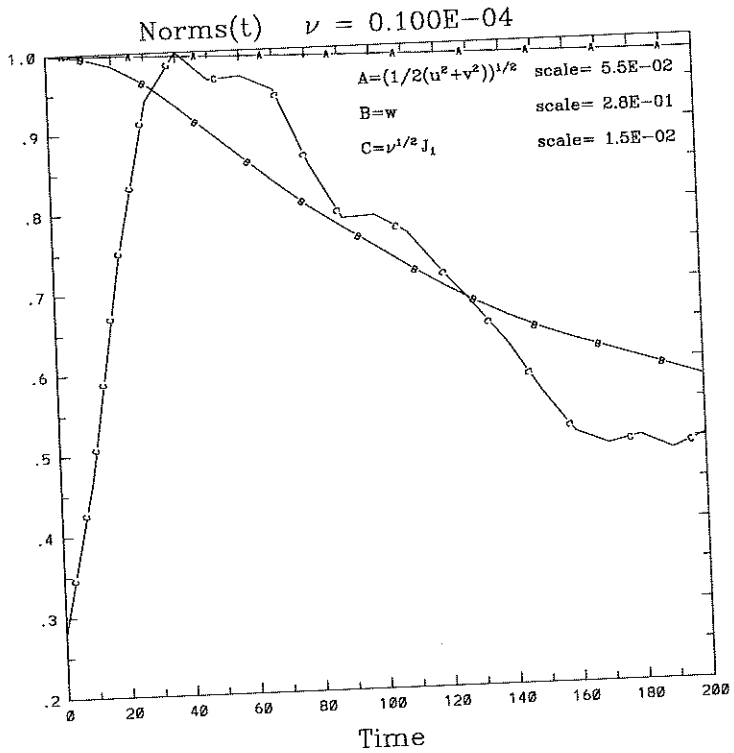

Figure 2: Unperturbed control run, spectra and norms.

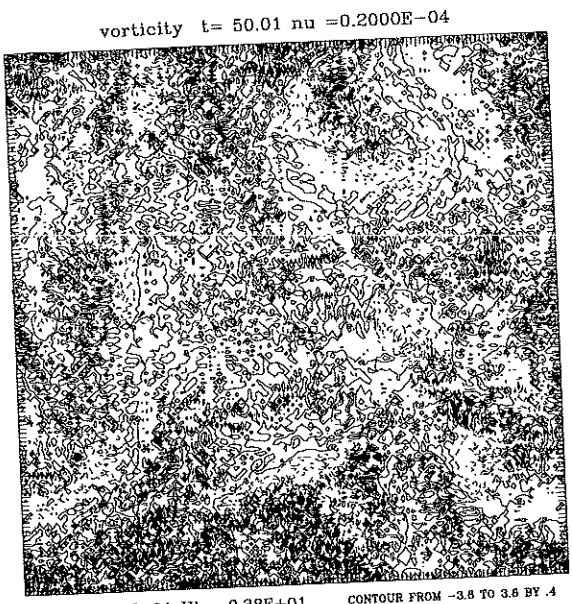

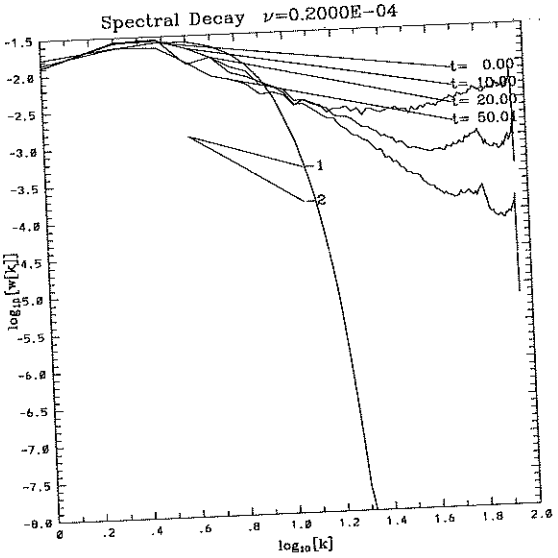

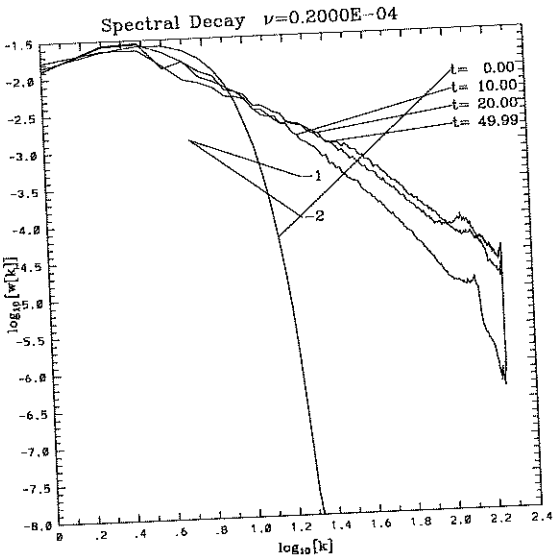

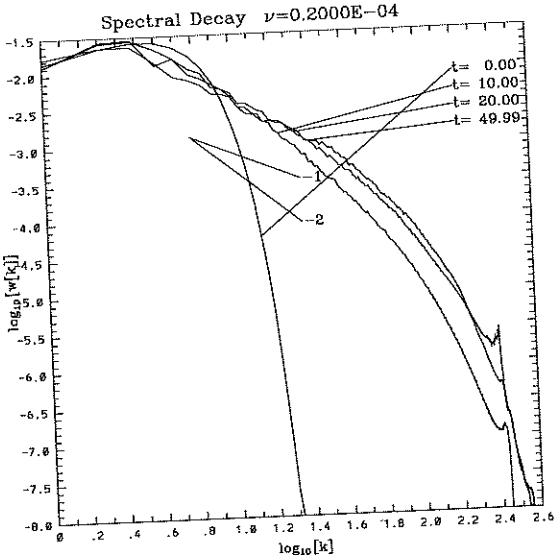

Figure 3: Solutions at time $t = 50.$ and vorticity spectra for $\nu = 2 \times 10^{-5}$ and $N = 128$ (top), $N = 256$ (middle), and $N = 512$ (bottom). The smallest scale estimate predicts a value of $N = 212$ grid points will resolve the flow.

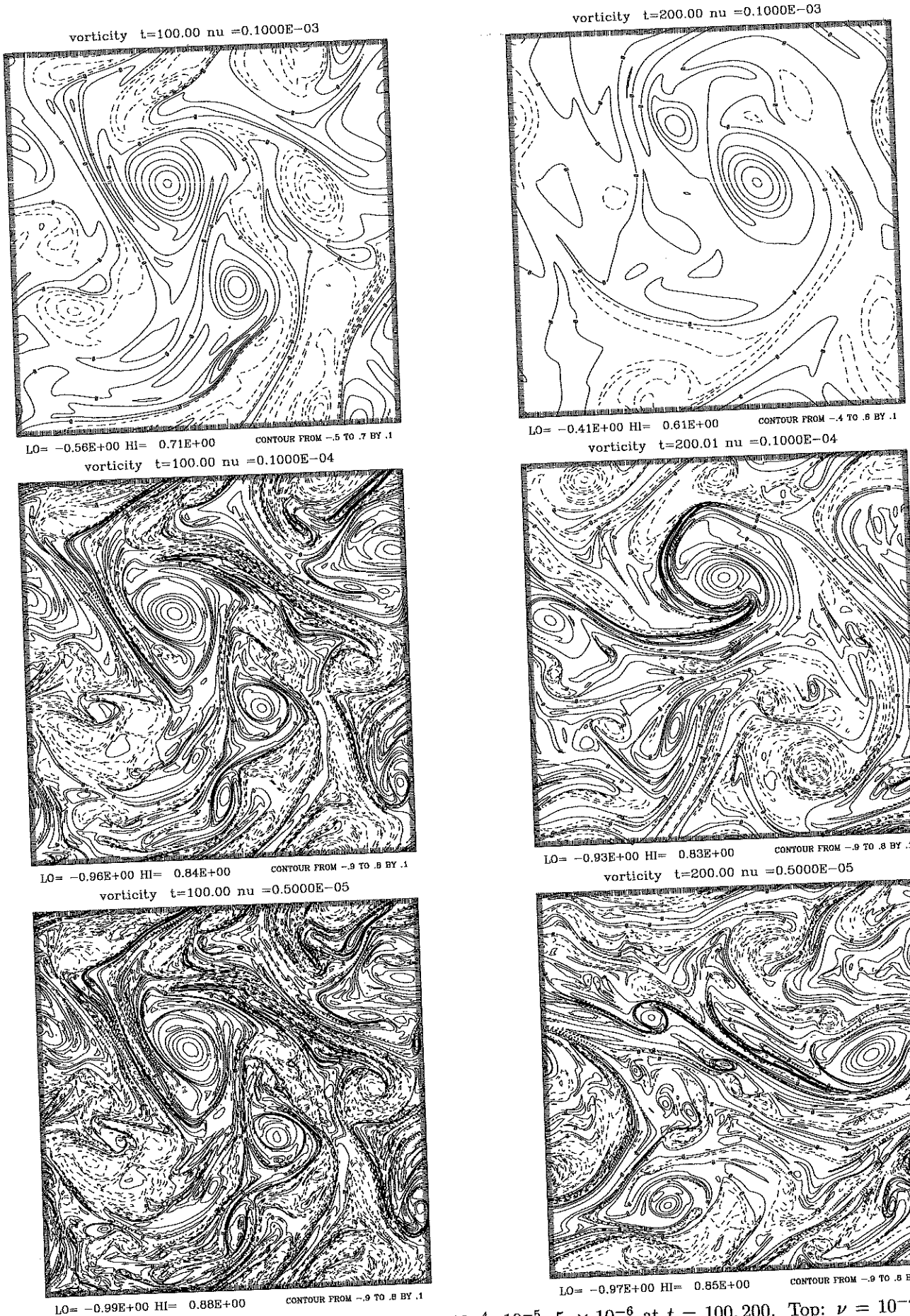

Figure 4: A comparison of the solutions for $\nu = 10^{-4}$, 10^{-5}, $5. \times 10^{-6}$ at $t = 100, 200$. Top: $\nu = 10^{-4}$, Middle $\nu = 10^{-5}$, bottom: $5. \times 10^{-6}$.

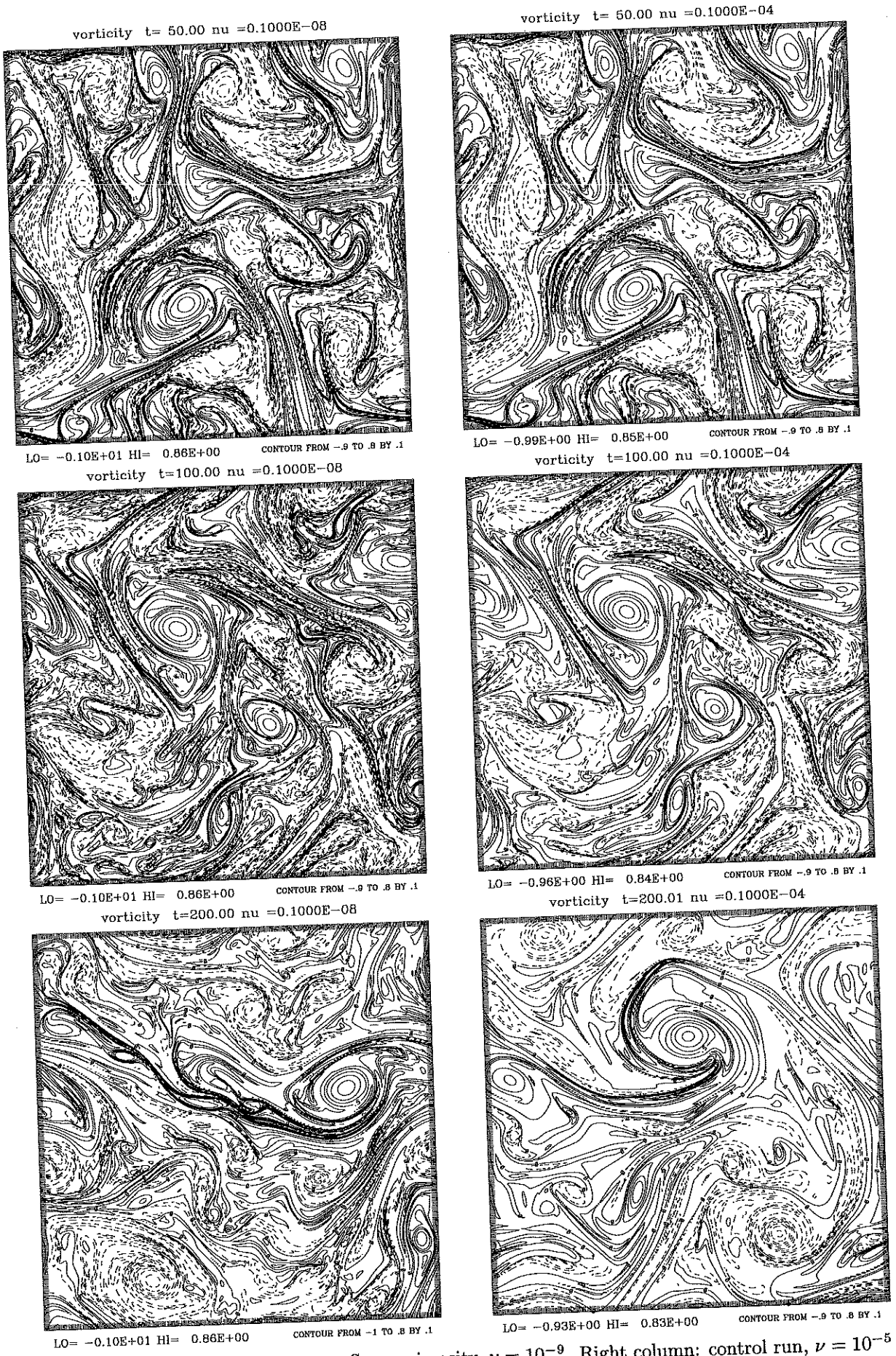

Figure 5: Left column: Super-viscosity, $\nu = 10^{-9}$. Right column: control run, $\nu = 10^{-5}$

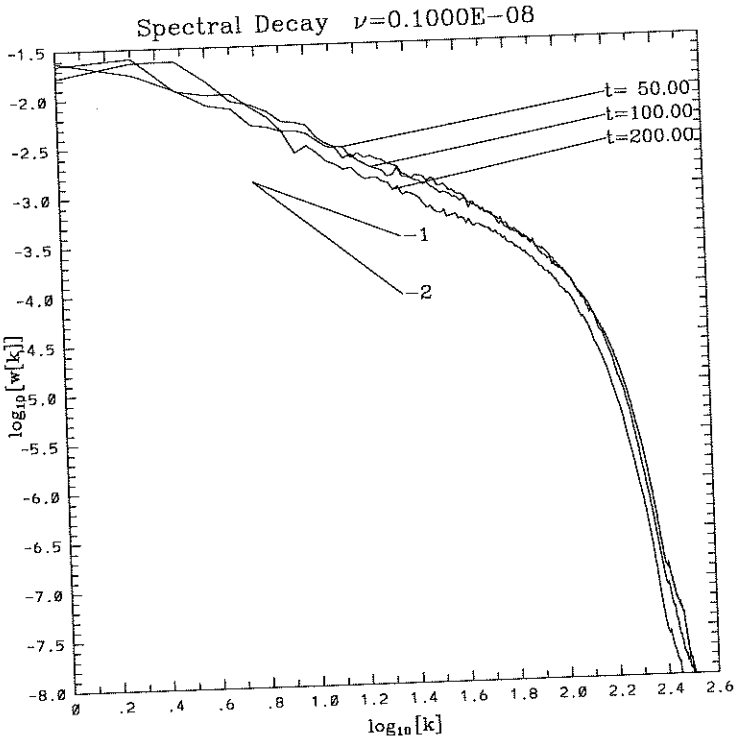

Figure 6: Super-viscosity, $\nu = 10^{-9}$

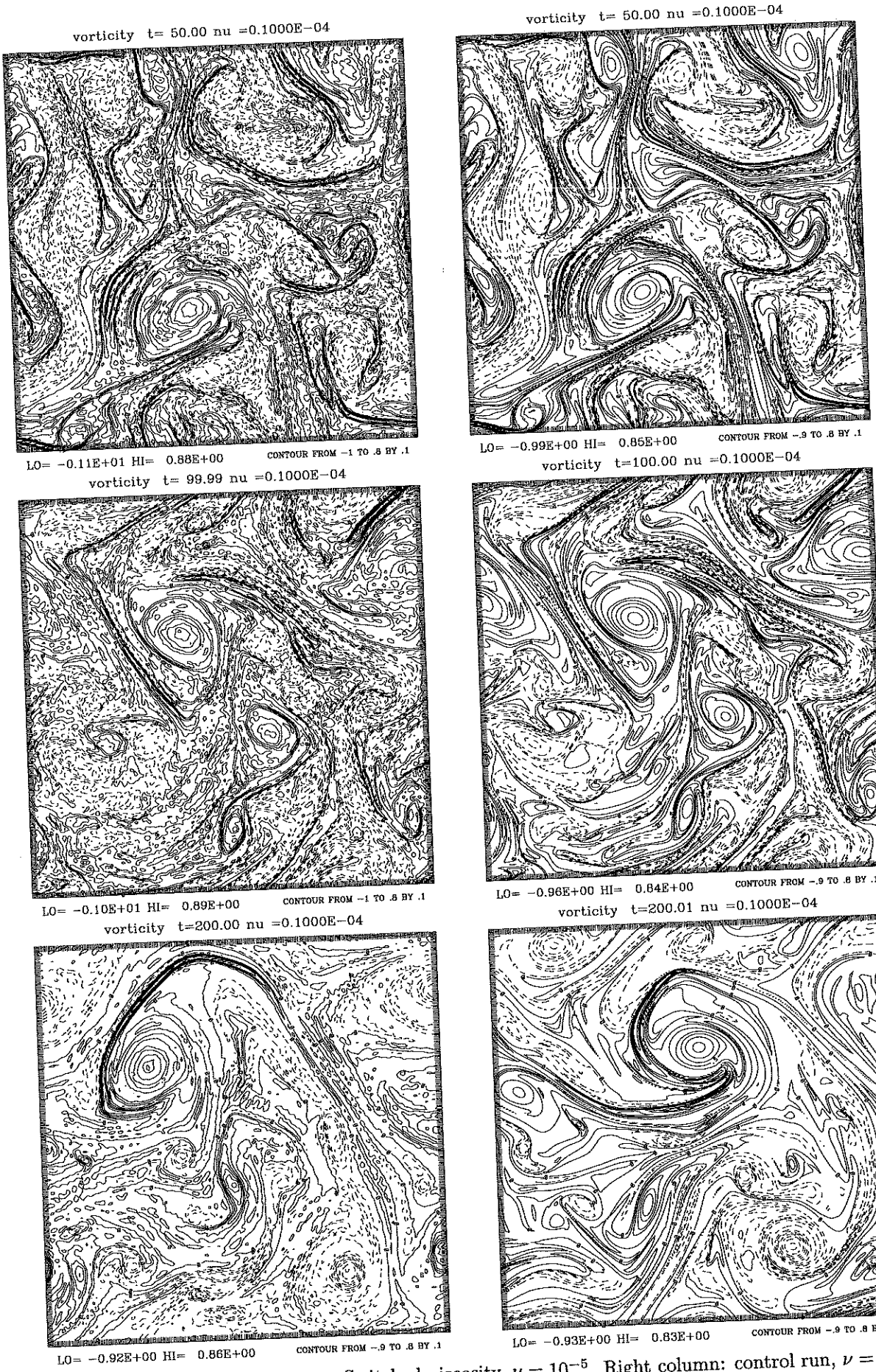

Figure 7: Left column: Switched-viscosity, $\nu = 10^{-5}$. Right column: control run, $\nu = 10^{-5}$

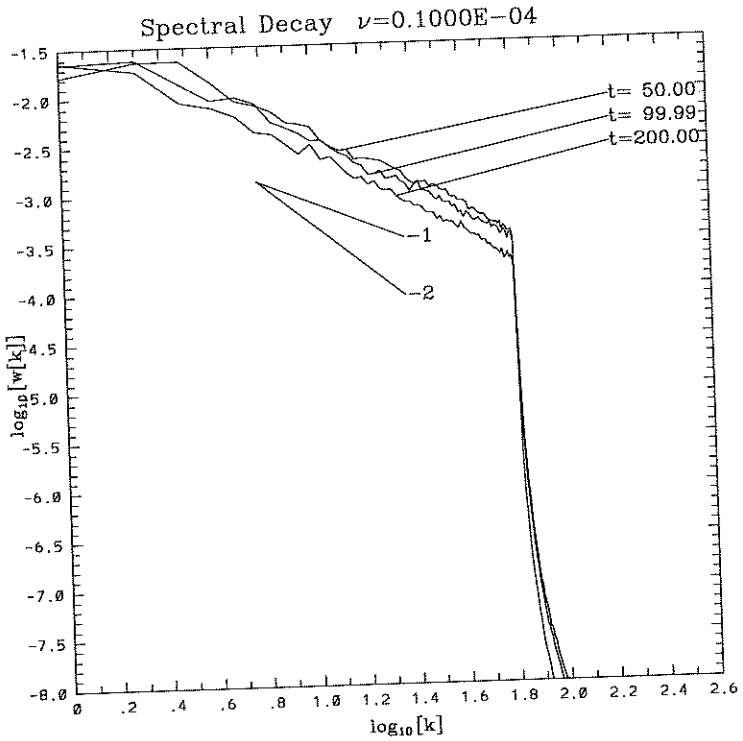

Figure 8: Switched-viscosity, switch at mode=64, $\nu = 10^{-5}$

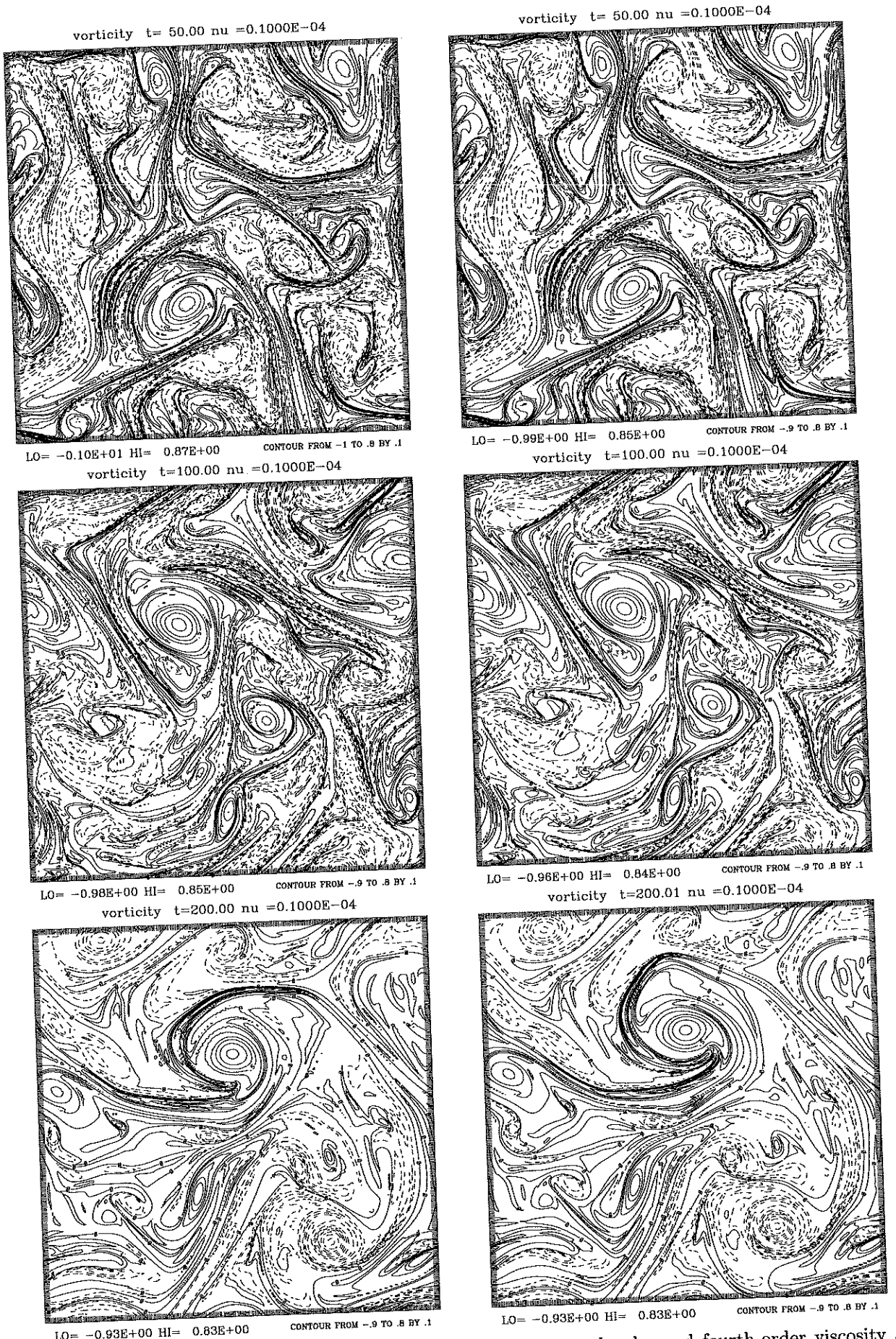

Figure 9: Left column: Switched-viscosity, switch between second-order and fourth-order viscosity at mode 128, $\nu = 10^{-5}$. Right column: control run, $\nu = 10^{-5}$

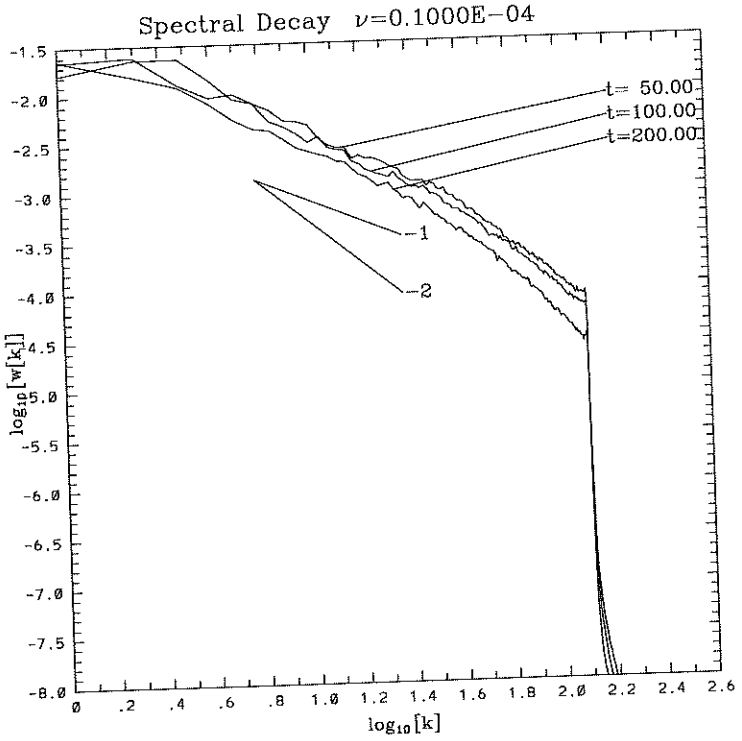

Figure 10: Switched-viscosity, switch between second-order and fourth-order viscosity at mode 128, $\nu = 10^{-5}$

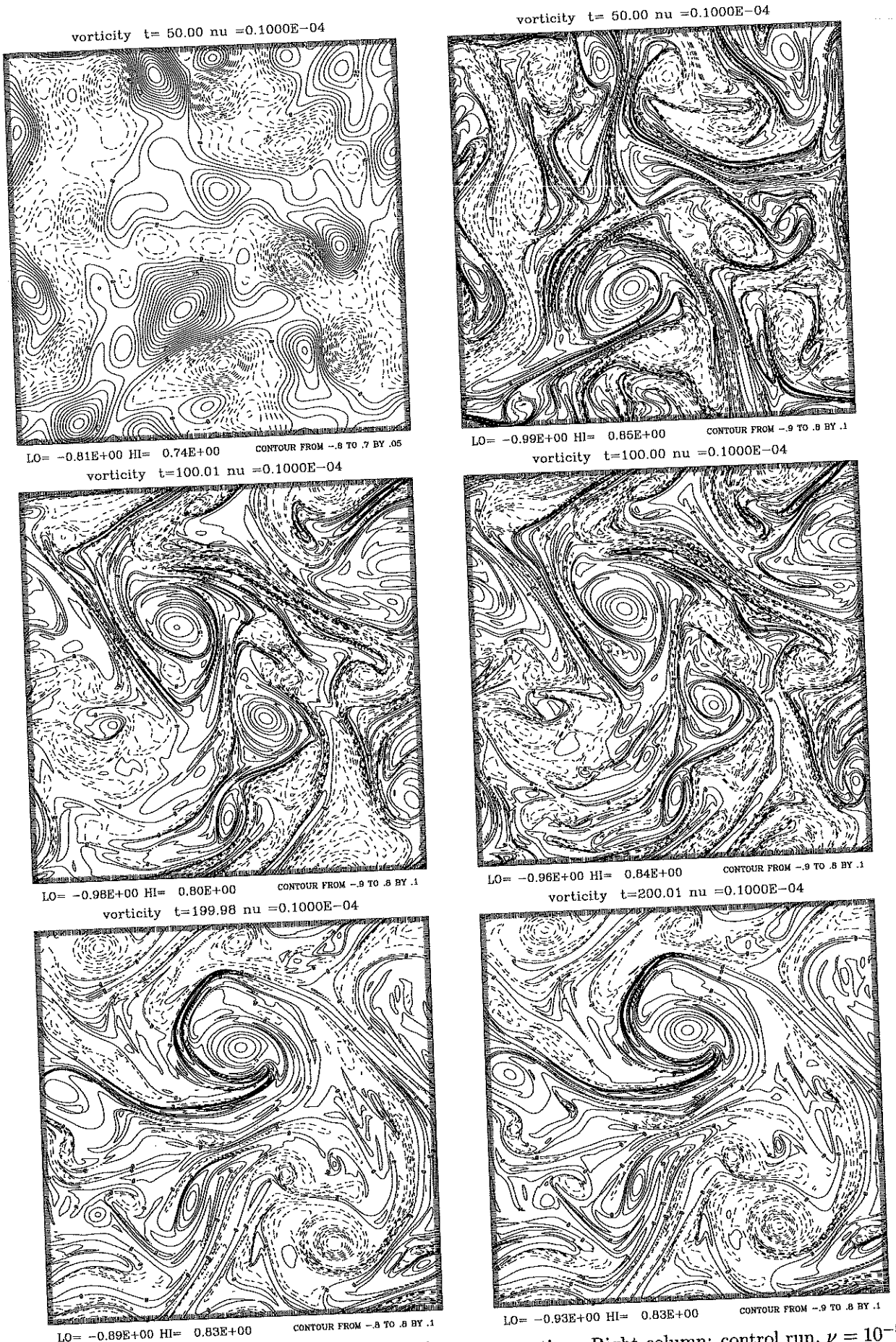

Figure 11: Left column: specify 8^2 modes over time. Right column: control run, $\nu = 10^{-5}$

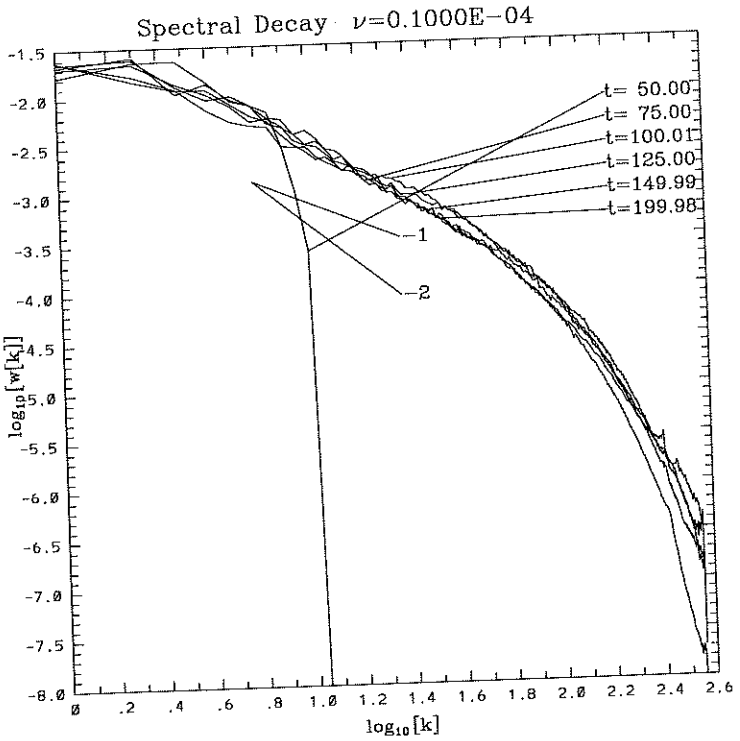

Figure 12: Specify 8^2 modes over time, all other modes initially set to zero, $\nu = 10^{-5}$.

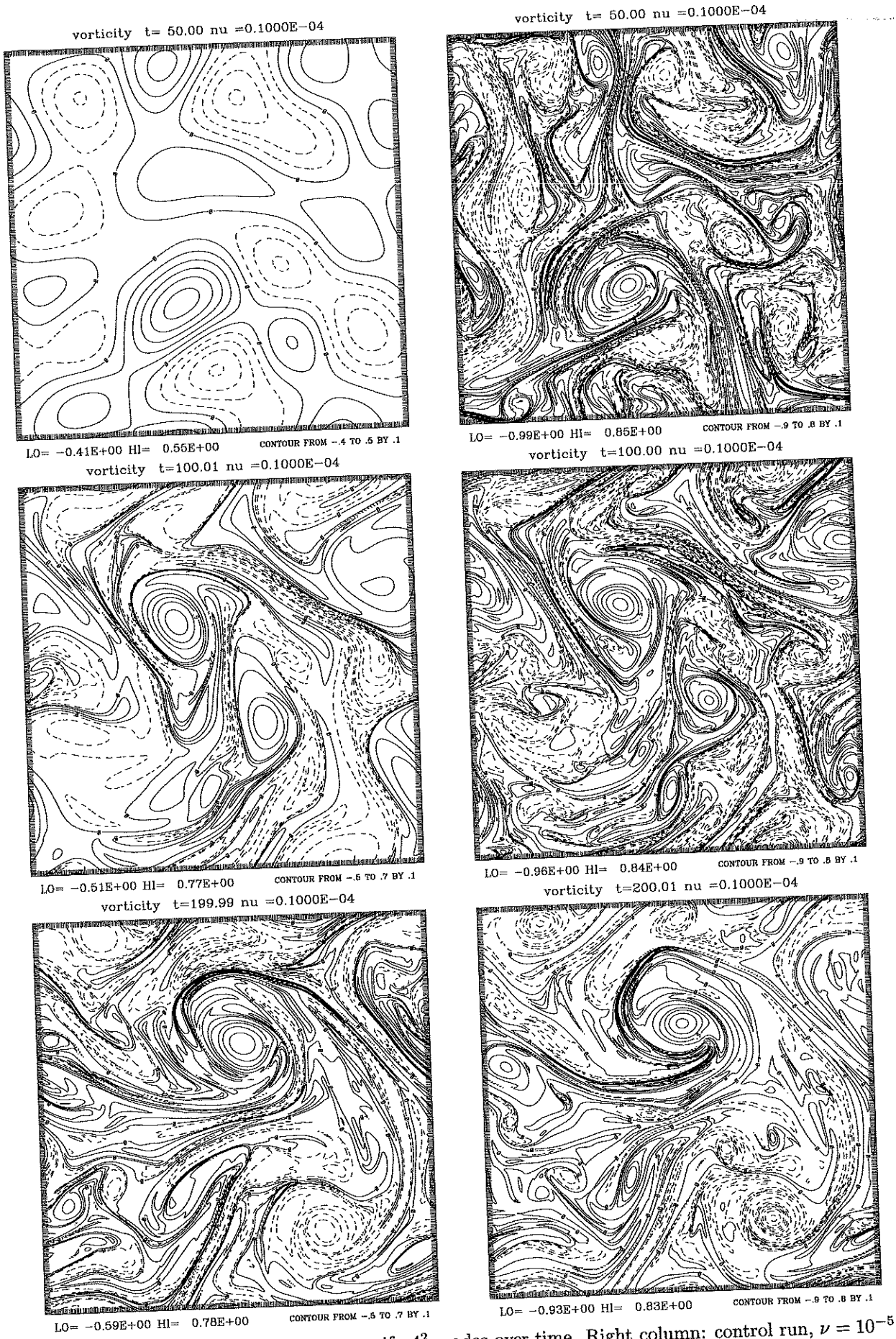

Figure 13: Left column: specify 4^2 modes over time. Right column: control run, $\nu = 10^{-5}$

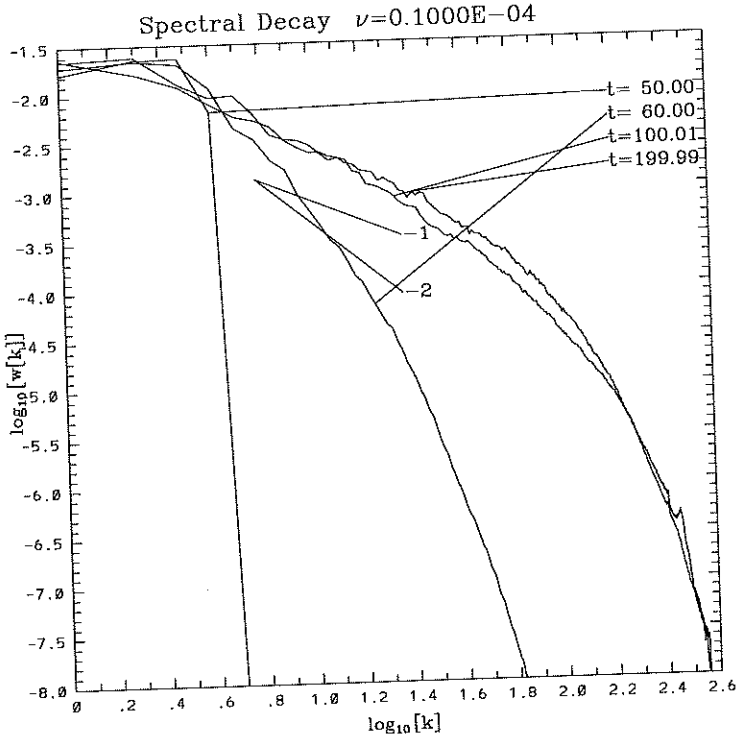

Figure 14: Specify 4^2 modes over time, all other modes initially set to zero, $\nu = 10^{-5}$.

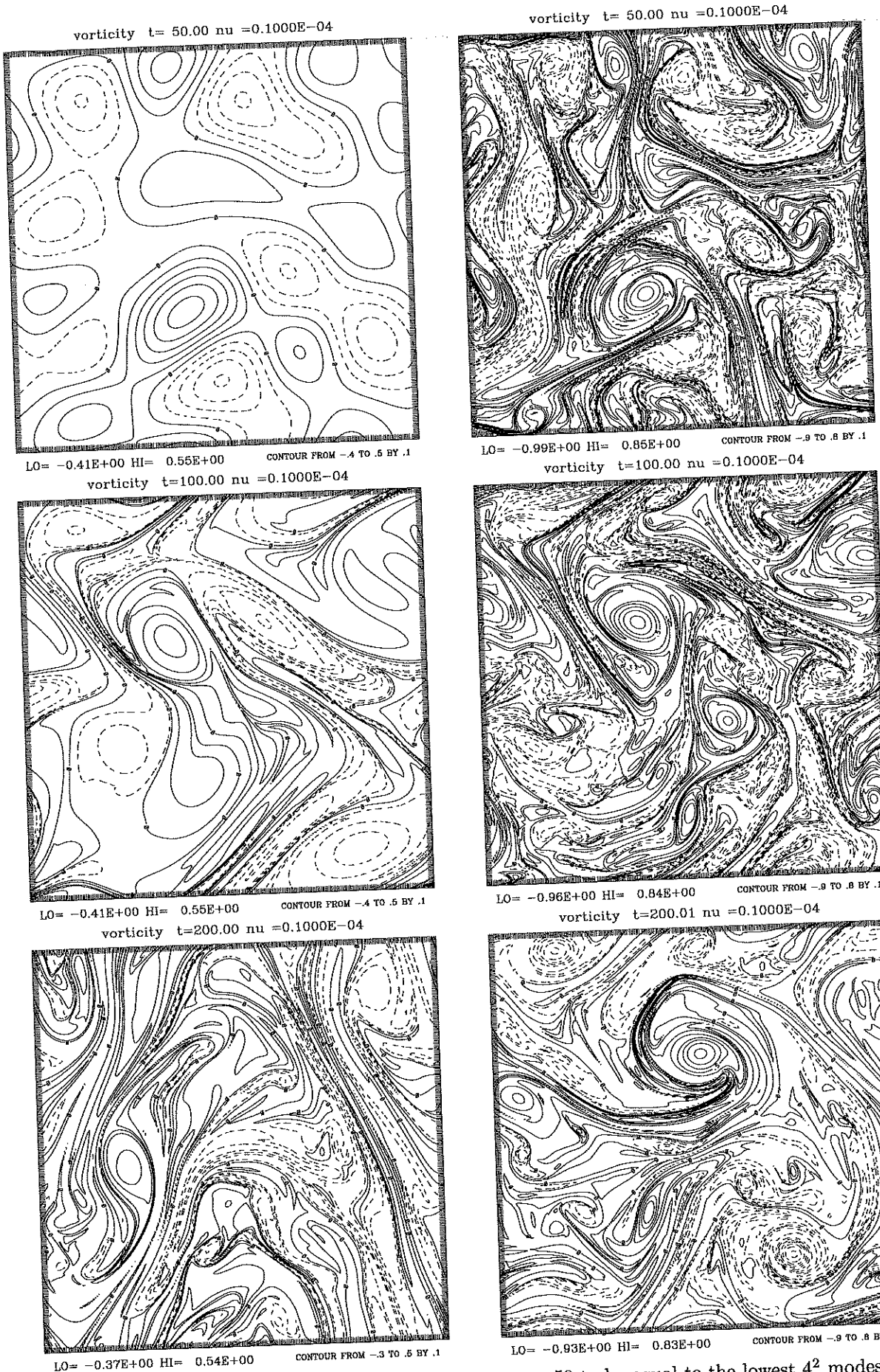

Figure 15: Left column: Specify the inital conditions at $t = 50$ to be equal to the lowest 4^2 modes from the control run. Do NOT specify these modes over time. Right column: control run, $\nu = 10^{-5}$

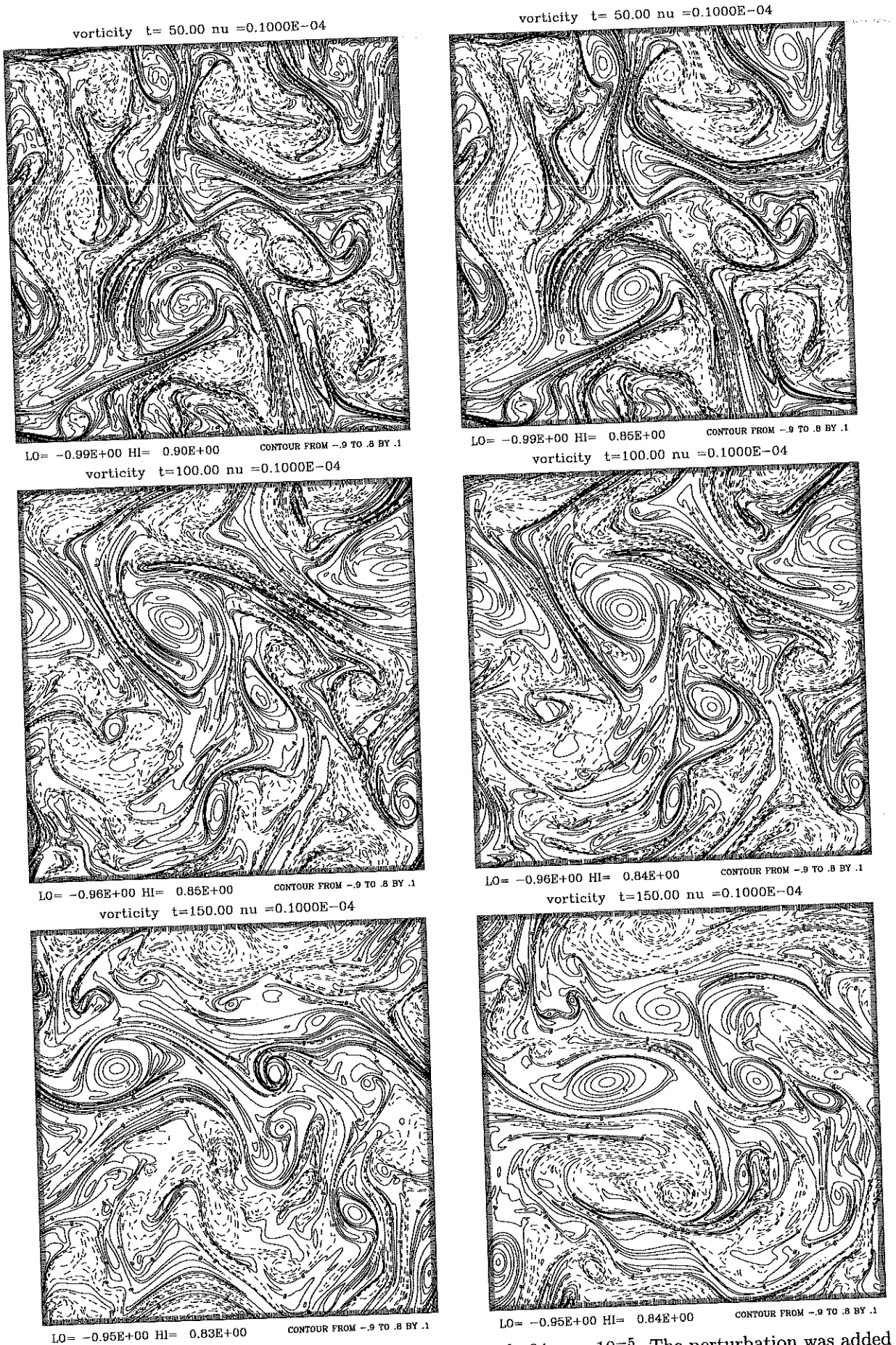

Figure 16: High frequency Gaussian perturbation at mode 64, $\nu = 10^{-5}$. The perturbation was added at time $t = 0$ and has an amplitude of 1. in physical space.

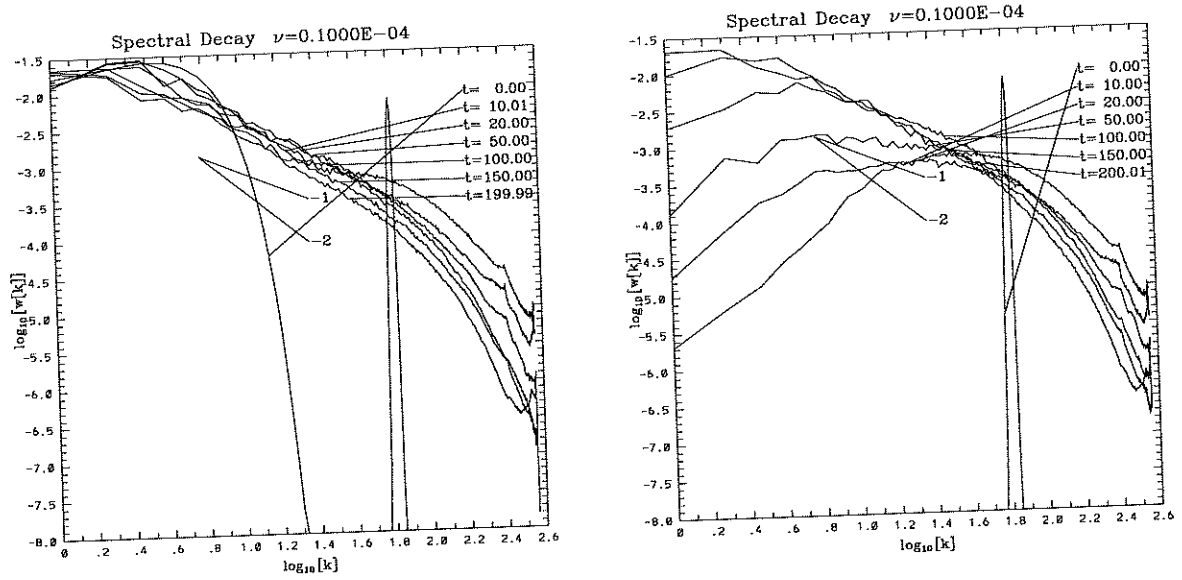

Figure 17: High frequency Gaussian perturbation at mode 64, added at $t = 0$, $\nu = 10^{-5}$. Left: spectrum of the perturbed solution. Right: spectrum of the difference between the perturbed solution and the control run.

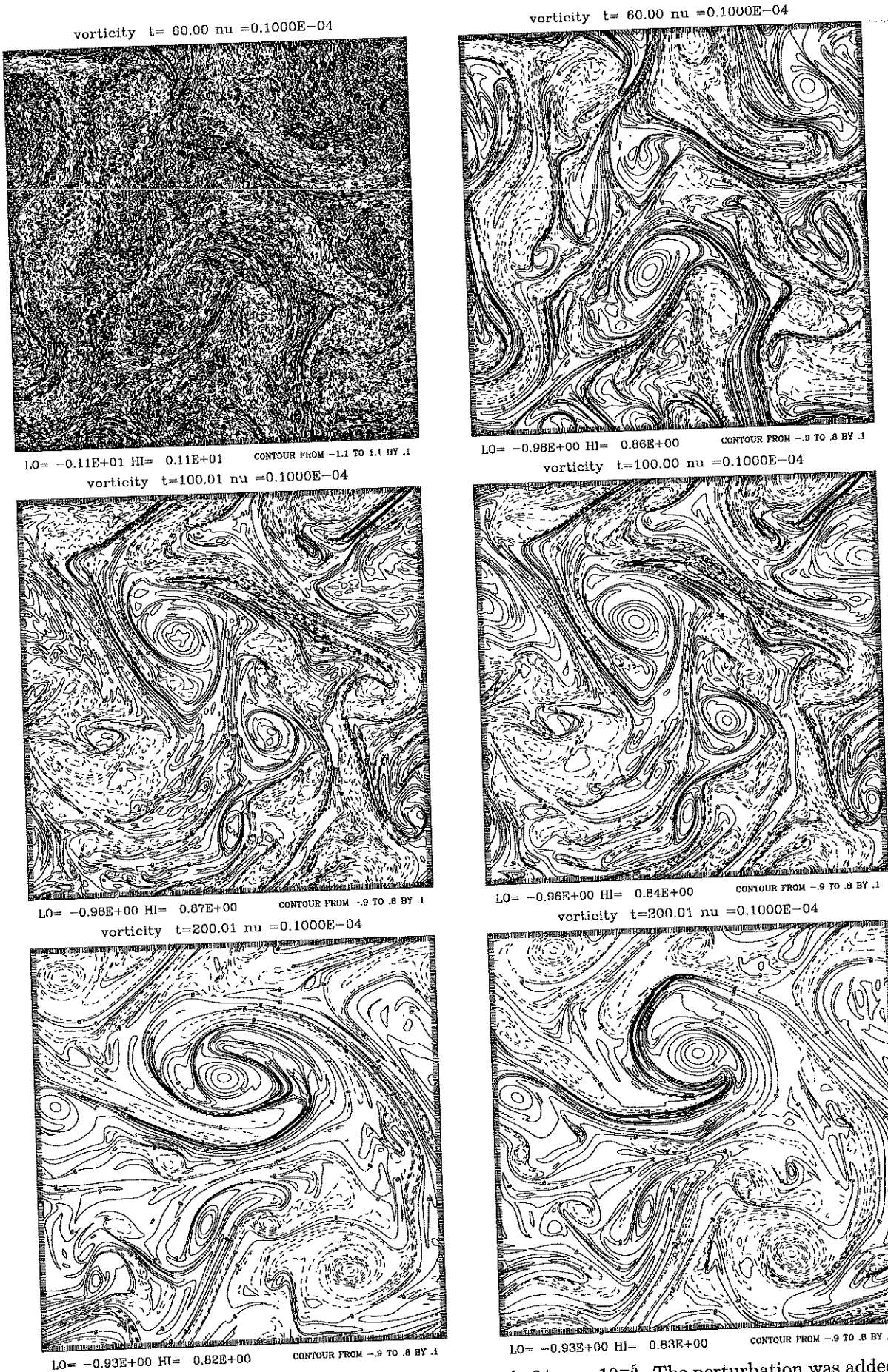

Figure 18: High frequency Gaussian perturbation at mode 64, $\nu = 10^{-5}$. The perturbation was added at time $t = 50$. and has an amplitude of 1. in physical space.

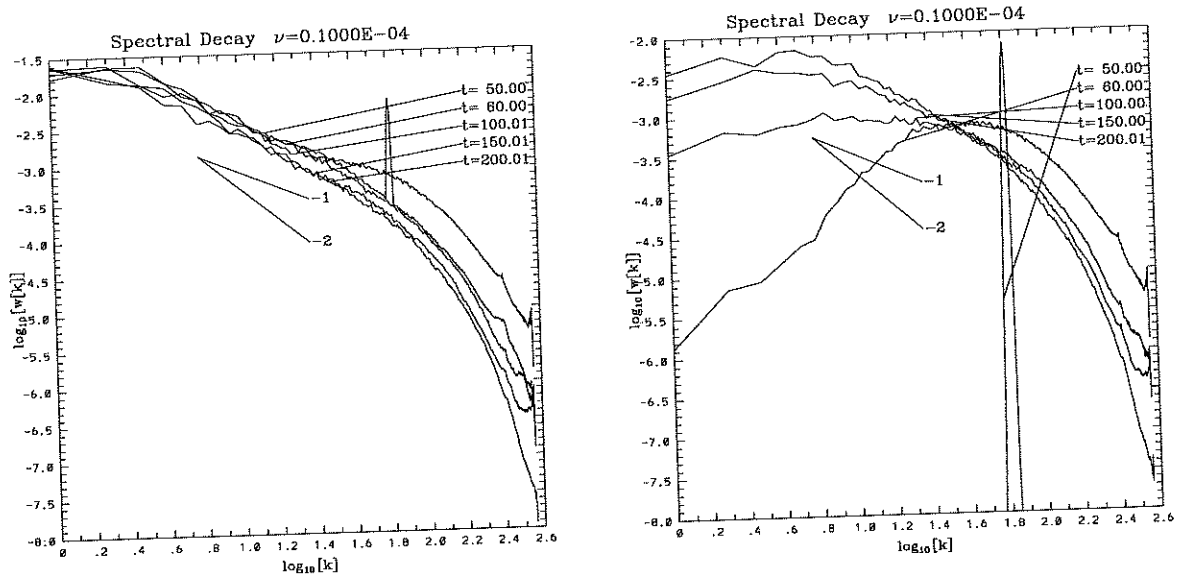

Figure 19: High frequency Gaussian perturbation at mode 64, added at $t = 0$, $\nu = 10^{-5}$. Left: spectrum of the perturbed solution. Right: spectrum of the difference between the perturbed solution and the control run.

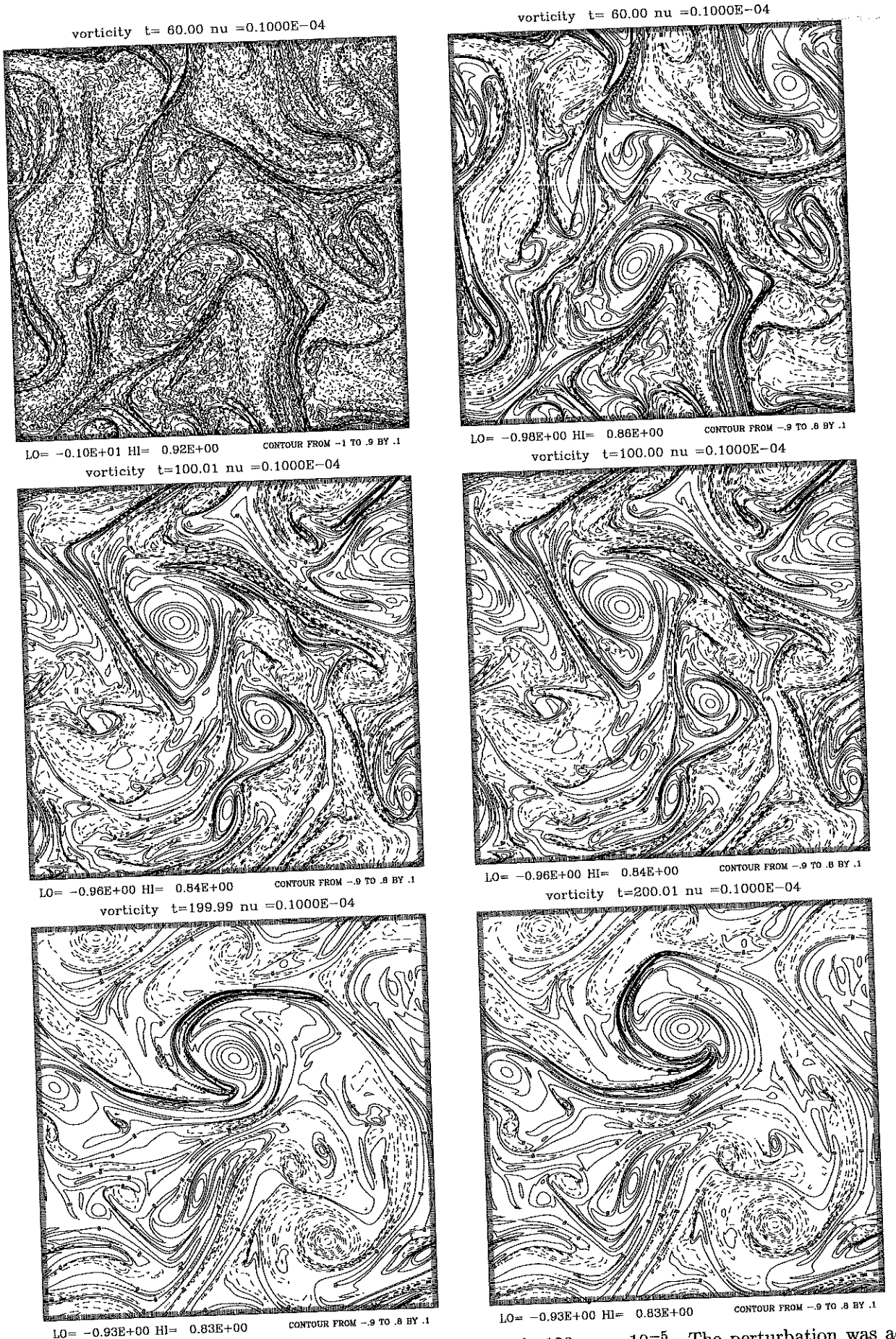

Figure 20: High frequency Gaussian perturbation at mode 128, $\nu = 10^{-5}$. The perturbation was added at time $t = 50.$ and has an amplitude of 1. in physical space.

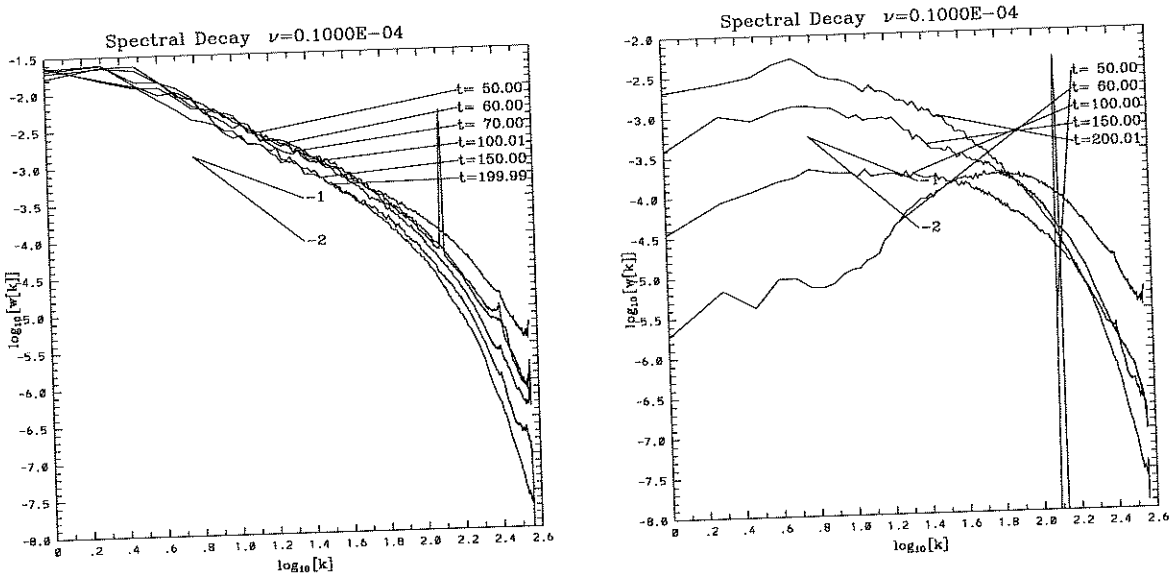

Figure 21: High frequency Gaussian perturbation at mode 128, $\nu = 10^{-5}$. Left: spectrum of the perturbed solution. Right: spectrum of the difference between the perturbed solution and the control run.

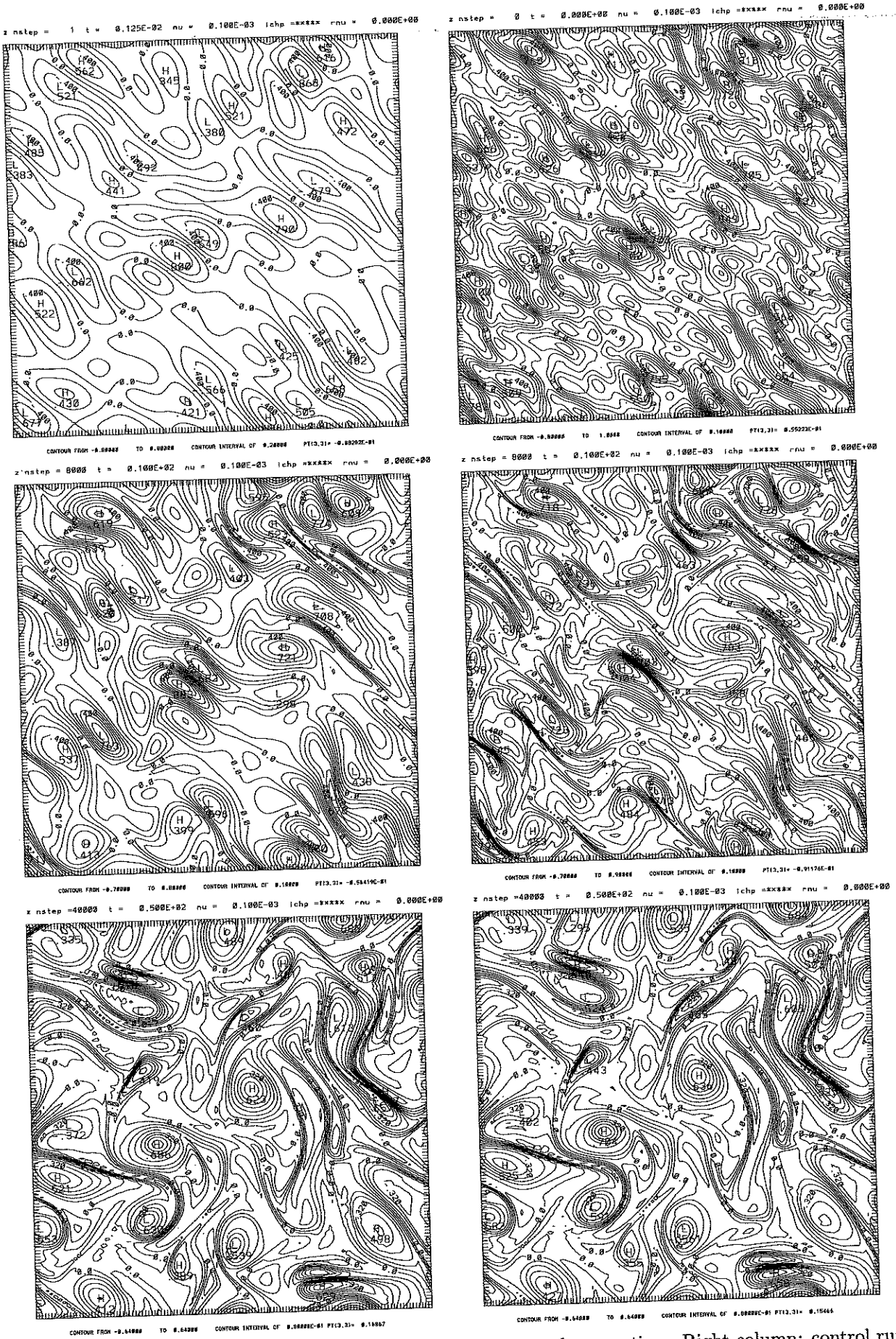

Figure 22: Shallow water equations, left column: specify 8 modes over time. Right column: control run, $\nu = 10^{-4}$